

# An improved simple shear apparatus for GCL internal and interface stress-displacement measurements

Hai Lin · Jianyong Shi · Xuede Qian ·  
Lingling Zhang

Received: 25 January 2013 / Accepted: 18 September 2013 / Published online: 2 October 2013  
© The Author(s) 2013. This article is published with open access at Springerlink.com

**Abstract** Geosynthetic clay liners (GCLs) have been widely used as a hydraulic barrier along with HDPE geomembrane (GM) in landfills. Both the internal and interface strengths of GCLs are very important for evaluating landfill stability. An improved simple shear apparatus used in this study does not force the shear failure to occur along a pre-determined plane. The composite specimens can fail along any interface or through shearing of the GCL internally. The displacement of each component of the specimen can also be measured during the tests. When non-woven geotextile side contacts textured GM (NWGT/GMX) and woven geotextile side contacts compacted clay layer (WGT/CCL) for a dry GCL, the failure interface can change from NWGT/GMX interface to WGT/CCL interface with the increases of the normal stresses. Conversely, when woven geotextile side contacts textured GM (WGT/GMX) and non-woven geotextile side contacts compacted clay layer (NWGT/CCL) for a dry GCL, the failure always occurs at the WGT/GMX interface for all applied normal stresses. The internal failure of the GCL did not occur when the normal stress increased up to 1,500 kPa for the GCL in dry condition.

**Keywords** Simple shear · GCL · Displacement · Interface strength · Peak strength

## Introduction

Geosynthetic clay liners (GCLs) are thin hydraulic barriers containing approximately 5 kg/m<sup>2</sup> of bentonite, sandwiched between two geotextiles or attached, with an adhesive, to a geomembrane (Bouazza 2002). As a hydraulic barrier, a GCL is an alternative to a compacted clay liner (CCL) and is widely used in the composite liner and cover systems of municipal solid waste (MSW) landfills (Qian et al. 2002). Considering the very low shear strength of the hydrated sodium bentonite, a large number of tests have been conducted to investigate the internal and interface shear strength properties of GCLs (Gilbert et al. 1996; Fox et al. 1998; Triplett and Fox 2001; Fox and Stark 2004; Zornberg et al. 2005; McCartney et al. 2009). Laboratory direct shear test results show a post-peak strength reduction for GCL interfaces and reinforced GCL internal face. GCL is generally laid dryly in the liner construction process, and then GCL can absorb moisture from the subbase soil with time (Anderson et al. 2012). Although full hydration represents the most critical state of GCL in base liner, dry or partial hydration is the most common state of GCL at work.

Translational failure along the liner system is a major concern in the design or construction of MSW landfill liners (Koerner and Soong 2000). For the multiple layered geosynthetic liner systems, there may be two or more critical potential sliding interfaces. For engineering application, it is worthwhile to determine the shear strength of a composite liner and the location of the failure surface within the liner. A typical MSW landfill liner system in China consists of a textured geomembrane (GM) underlain

---

H. Lin (✉) · J. Shi  
Key Laboratory of Ministry of Education for Geomechanics and Embankment Engineering, Geotechnical Research Institute, Hohai University, Nanjing 210098, China  
e-mail: yantulinhai@hhu.edu.cn

X. Qian  
Michigan Department of Environmental Quality, Office of Waste Management and Radiological Protection, 525 West Allegan, Lansing, MI 48933, USA

L. Zhang  
College of Harbour, Coastal and Offshore Engineering, Hohai University, Nanjing 210098, China

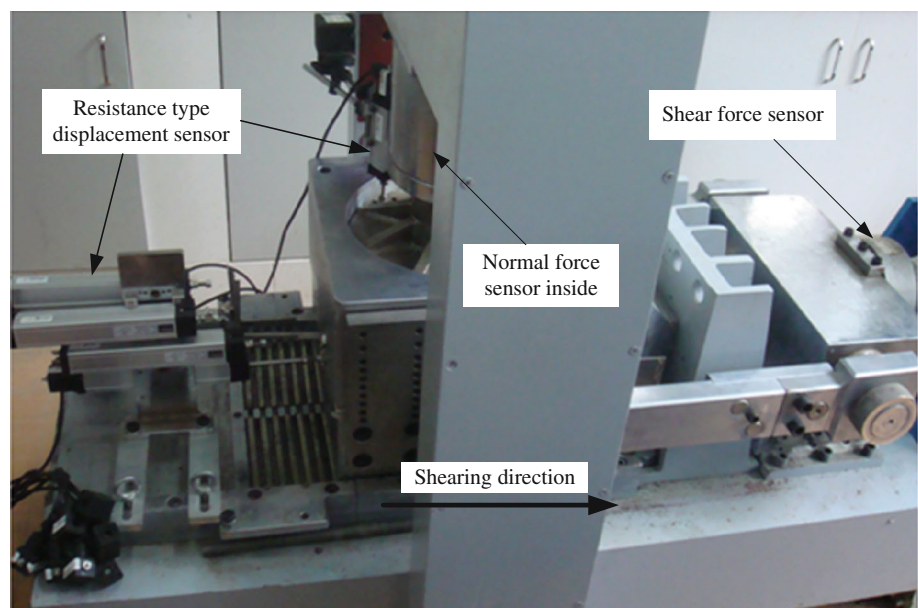
by a needle-punched GCL, which in turn is underlain by a compacted soil layer ( $k < 10^{-5}$  cm/s; CJJ 113-2007 2007). Recently, shear strength of composite liner system attracted the attention of scholars. Eid (2011) conducted torsional ring shear tests of a GM/GCL/silty clay liner without forcing failure to occur through a pre-determined plane. The torsional ring shear tests showed that failure of the composite liner system could be controlled by different failure modes depending on the magnitude of normal stress ( $\sigma_n$ ) and the comparative values of the GCL interface and internal shear strength (Eid 2011). The critical failure face changed from the interface between needle-punched GCL and silty clay ( $\sigma_n < 75$  kPa) to interface between GCL and textured GM ( $\sigma_n = 100 \sim 250$  kPa), and then to GCL internal ( $\sigma_n = 300, 350$  and  $400$  kPa) as normal stress increases. Fox and Ross (2011) conducted large direct shear tests for GM/GCL composite interfaces without forcing failure plane. Large direct shear tests showed that the failure face would change from the interface to GCL internal as normal stress increases (Fox and Ross 2011). In the tests of Eid (2011) and Fox and Ross (2011), GCL internal displacement and interface displacement between GCL and its adjacent materials could not be obtained because the test machine was unable to measure the displacement of GCL. This paper introduces an improved simple shear apparatus and corresponding testing method for a composite liner containing GCL. Through the testing method, GCL internal displacement and interface displacements between GCL and its adjacent materials can be measured during shearing. Detailed analyses about shear behavior of a composite liner containing GCL can then be obtained.

## Apparatus and test materials

Simple shear tests were performed for various GCL composite liner systems by using a large improved simple shear apparatus in this research (Fig. 1). The diameter of the specimens is 300 mm. The normal stress is applied by a hydraulic oil cylinder and controlled by a computer. The specimens can be sheared under a large range of the normal stresses. The maximum normal stress can be up to 2.8 MPa. The shearing system is powered by two stepper motors that rotate two lead screws and pull the lower shear box forward at a constant displacement rate. The force sensors are installed at the vertical axial direction and the lateral shear direction of the apparatus, respectively. The shearing displacement can be measured by the displacement sensors. The values of the forces and displacements can be automatically recorded by a computer during the tests. Two rows of free-rolling, stainless-steel balls were installed between the lower shear box and the bottom plane to minimize the friction resistance due to the applied normal stress.

Several thin steel rings were made with a thickness of 1 or 2 mm and an inside diameter of 300 mm. These rings are attached to the upper and lower sides of the GCLs geotextiles to measure the internal and interface displacements of the GCL during the tests. The maximum shearing displacement can occur at any weakest interface or internal face in the composite liner system by using this simple shear apparatus. In order to investigate the peak shear stress for different layers of the composite liner system, a horizontal displacement of 35 mm was selected to be used in the tests.

**Fig. 1** Large direct shear apparatus (photo courtesy of the writers)



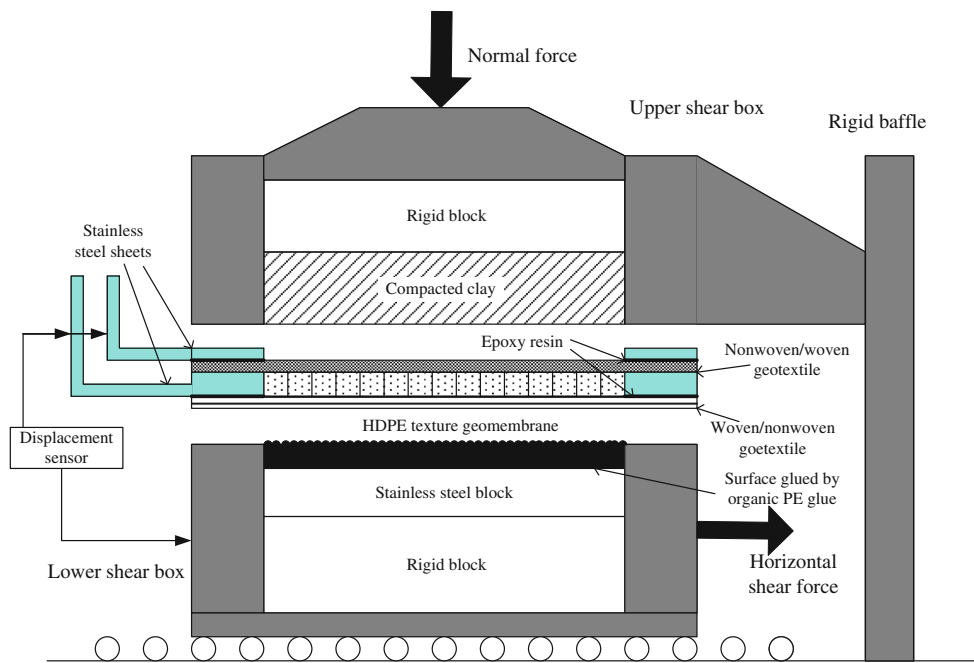


**Fig. 2** Schematic diagram for set-up of the simple shear tests

The smooth side of the GM was glued to a rigid steel block placed in the lower shear box. From top to bottom, a set of the testing specimens consists of the compacted clay layer, GCL, and GM. Two thin stainless-steel rings with an inside diameter of 300 mm and the same outside dimensions as the upper and lower shear boxes were glued to the upper and lower geotextiles of the GCL, respectively, by using epoxy resin, as shown in Fig. 2. The internal and interface displacements of the GCL can be obtained by measuring the lateral movements of the lower shear box and the two thin rings.

The friction forces may be mobilized by the interface between the frame of the upper shear box and upper thin ring, the interface between the upper geotextile of the GCL and the lower thin ring, and the interface between the lower geotextile of the GCL and the frame of the lower shear box, which may affect the testing results. However, the calibration test results show that the maximum friction forces mobilized by these interfaces will not exceed 0.2 kN under the weight of the upper shear box. Comparing with the measured peak shear force, the experimental errors caused by the friction forces will be <5 % at  $\sigma_n = 100$  kPa and <2 % at  $\sigma_n = 300$  kPa, respectively. The errors will decrease with the increase of the normal stress. In that case, the influence of the friction forces for the testing results can be ignored.

The GCL used in tests was supplied by a GCL company of China and consists of approximate 5 kg/m<sup>2</sup> of sodium bentonite encapsulated between a woven silt-film polypropylene geotextile and a non-woven, needle-punched polypropylene geotextile, which are needle-punched together.

The liquid limit of the bentonite in the GCL is 240 % and the swell index is 25 ml/2 g. Other geotechnical parameters of the GCL are listed in Table 1. A 1.5-mm one-side textured HDPE geomembrane was used in the tests. Local clay was used in the tests with the optimum water content of 16 % and the maximum dry density of 17.7 kN/m<sup>3</sup>.

Unlike the direct shear apparatus, the large improved simple shear apparatus used in this study does not force the shear failure to occur along a pre-determined plane. The composite specimens can fail along the GCL woven or non-woven geotextile side/textured geomembrane interface, the GCL non-woven or woven geotextile side/compacted clay interface, or through shearing of the GCL internally. Simultaneous shearing of a composite liner specimen that contains several components affected by the same testing conditions helps in simulating the field conditions more rather than testing shear strength of each interface individually. Another advantage of this simple shear apparatus is that the displacement of each component of a composite liner specimen can be measured during the tests, which is impossible for the torsional ring shear apparatus.

### Test procedure

#### Specimen preparation

ASTM D 6243-09 (2009) recommends that GCLs should be tested in direct shear with a minimum specimen dimension of 300 mm. First of all, GCL specimens were

**Table 1** Geotechnical parameters of geosynthetics

Geosynthetic clay liner (GCL)	Thickness (mm)	Peel strength (N/10 cm)	Mass/area (g/m <sup>2</sup> )	Swell index (ml/2 g)	Tensile strength (N/10 mm)	Vertical permeability coefficient (cm/sec)
	6	114	5,000	25	1,560	$4.32 \times 10^{-12}$
Texture geomembrane (GM)	Thickness (mm)	Texture height (mm)	Density (g/cm <sup>3</sup> )	Yield strength (N/mm)	Yield elongation (%)	Puncture strength (N)
	1.5	0.26	0.94	27	12	521

cut to 370 × 370 mm size. Except for the center 300-mm diameter circle area, the needle-punched reinforced fibers of the GCL specimen were cut and removed. Then, the bentonite beyond the 300-mm diameter circle area was removed carefully. Two thin stainless-steel rings with an inside diameter of 300 mm were glued to the non-woven geotextile side and to the woven geotextile side of GCL, respectively, by using epoxy resin, as shown in Fig. 2. The GCL specimen was maintained at least 24 h before testing to allow the epoxy resin to gain adequate strength. The smooth side of the GM was glued at a circle metal block by using special organic PE glue and then set in the lower shear box.

The steel blocks were placed under the GM in the lower shear box to avoid vertical displacement. This also ensures the textured surface of the GM to stay on the top of the lower shear box under the high normal stresses during the tests. The prepared GCL specimen was placed over the textured side of the GM. The upper shear box with the compacted clay was then placed over the GCL specimen. Some Vaseline was smeared on the inside wall of the upper shear box to reduce the friction between compacted clay and the apparatus. Preparation of clay sample was according to ISO/TS 17892-10-2004 (2004). The clay was compacted to its maximum dry density (17.7 kN/m<sup>3</sup>) in the upper shear box by two layers. The tests were divided into two groups. Test Group A is the non-woven geotextile side of the GCL that contacted the textured geomembrane (NWGT/GMX) and the woven geotextile side of the GCL contacted the compacted clay layer (WGT/CCL). Test Group B is the woven geotextile side of the GCL that contacted the textured geomembrane (WGT/GMX) and the non-woven geotextile side of the GCL contacted the compacted clay layer (NWGT/CCL). For Test Group A, the specimens were sheared at the normal stresses of 50, 100, 200, 300, 400, 500, 800, 1,300, and 1,500 kPa, respectively. For Test Group B, the specimens were sheared at the normal stresses of 100, 300, 500, 800, and 1,300 kPa, respectively.

#### Vertical loading and shearing

Settlement stabilization for the compacted clay layer placed in the upper shear box can be obtained in 6 h after applying normal stress. The shearing displacement rate can affect the test results of both the internal and interface strengths of the GCL. However, the effect of the shearing displacement rate can be neglected for dry GCLs when the displacement rate ( $R$ ) is less than 1 mm/sec (Eid and Stark 1997, 1999; Ross et al. 2011). In order to eliminate the effect of the shearing displacement rate on the test results, a shearing displacement rate of 0.3 mm/min was selected in this research. A total of three shearing displacements

**Table 2** Summary of test results

Test group	Normal stress (kPa)	Peak strength (kPa)	Total horizontal displacement at $t_p$ (mm)	Failure surface	Displacement of critical failure surface at $t_p$ (mm)
A	50	45.3	2.5–2.8	NWGT/GMX	1.6–2.5
A	100	60.8	7–9	NWGT/GMX	3.5–4.5
A	200	117.4	14–15	NWGT/GMX	4.5–5.5
A	300	169.8	14–15	NWGT/GMX	4.5–5.5
A	400	236.3	–	WGT/CCL	–
A	500	287.2	17–19	NWGT/GMX	5.5–6.5
A	800	377.7	–	WGT/CCL	–
A	1,300	592.8	–	WGT/CCL	–
A	1,500	611.2	–	WGT/CCL	–
B	100	60.8	3–4	WGT/GMX	1.5–2.0
B	300	144.30	4–5	WGT/GMX	1.8–2.6
B	500	241.92	10.7–10.9	WGT/GMX	5.9–6.2
B	800	349.43	10.1–10.3	WGT/GMX	5.8–5.9
B	1,300	615.40	13.9	WGT/GMX	6.5

Series A refers to tests when GCL non-woven side contacts textured GM, and series B refers to tests when GCL woven side contacts textured GM.  $t_p$  is the moment peak strength is reached

was recorded by using the computer during the tests. They are the displacement of the lower shear box where the GM is fixed ( $\delta_1$ ), the displacement of the lower thin ring attached on the lower geotextile of the GCL ( $\delta_2$ ), and the displacement of the upper thin ring attached on the upper geotextile of the GCL ( $\delta_3$ ). The value of  $\delta_1$  represents the total shearing displacement of the composite liner system used in the tests ( $\Delta_1$ ), which is similar to the study of Fox and Ross (2011). The interface displacement between the textured geomembrane and the lower surface of the GCL ( $\Delta_2$ ) can be obtained from the difference of the displacement of the lower shear box and the displacement of the lower thin ring, i.e.,  $\delta_1 - \delta_2$ . The internal displacement of the GCL ( $\Delta_3$ ) can be calculated from the difference of the displacement of the lower thin ring and the displacement of the upper thin ring, i.e.,  $\delta_2 - \delta_3$ . The value of  $\delta_3$  represents the interface displacement between the upper surface of the GCL and the compacted clay layer ( $\Delta_4$ ).

**Test results**

The shear stress and the displacement of each internal face and interface in the liner system were recorded during the tests. Table 2 provides a summary of the test results. The detailed analysis is provided as follows.

**Displacement behavior**

The relationships between displacements and time for each internal face and interface of the tested liner systems for Test Groups A and B are shown in Figs. 3 and 4,

respectively. The curves of the total displacement ( $\Delta_1$ ) versus time appear linear under all normal stresses as shown in both Figs. 3 and 4. It can be found in Figs. 3 and 4 that if the displacement of an interface in the liner system can continuously increase with time under a certain normal stress during the test, this interface must be the critical failure interface (i.e., the weakest interface) of the liner system under this normal stress.

For Test Group A, it can be seen in Fig. 3 that the critical failure face changes from the interface of NWGT/GMX to the interface of WGT/CCL with increase of the normal stress. The critical failure face is located at the interface of NWGT/GMX for  $\sigma_n = 50, 100, 200, 300,$  and  $500$  kPa. The critical failure face is located at the interface of WGT/CCL for  $\sigma_n = 400, 800, 1,300,$  and  $1,500$  kPa. Note that the critical failure face shifts from the interface of NWGT/GMX to the interface of WGT/CCL for  $\sigma_n = 400$  kPa, as shown in Fig. 3e; and then the critical failure face shifts back from the interface of NWGT/GMX again for  $\sigma_n = 500$  kPa, shown in Fig. 3f. The critical failure face is stably located at the interface of WGT/CCL when the normal stress is greater than 500 kPa. This phenomenon was confirmed by repeated tests. The strength variability of the interfaces of multilayer geosynthetic liner systems may cause such phenomena (Dixon et al. 2006). It also indicates that the shear strengths of the interfaces of NWGT/GMX and WGT/CCL are very close when the normal stress changes between 400 and 500 kPa. Thus, there is a critical range of the normal stress for Test Group A (i.e.,  $\sigma_n = 400 \sim 500$  kPa) in which the failure may occur at the interface of either NWGT/GMX or WGT/CCL.

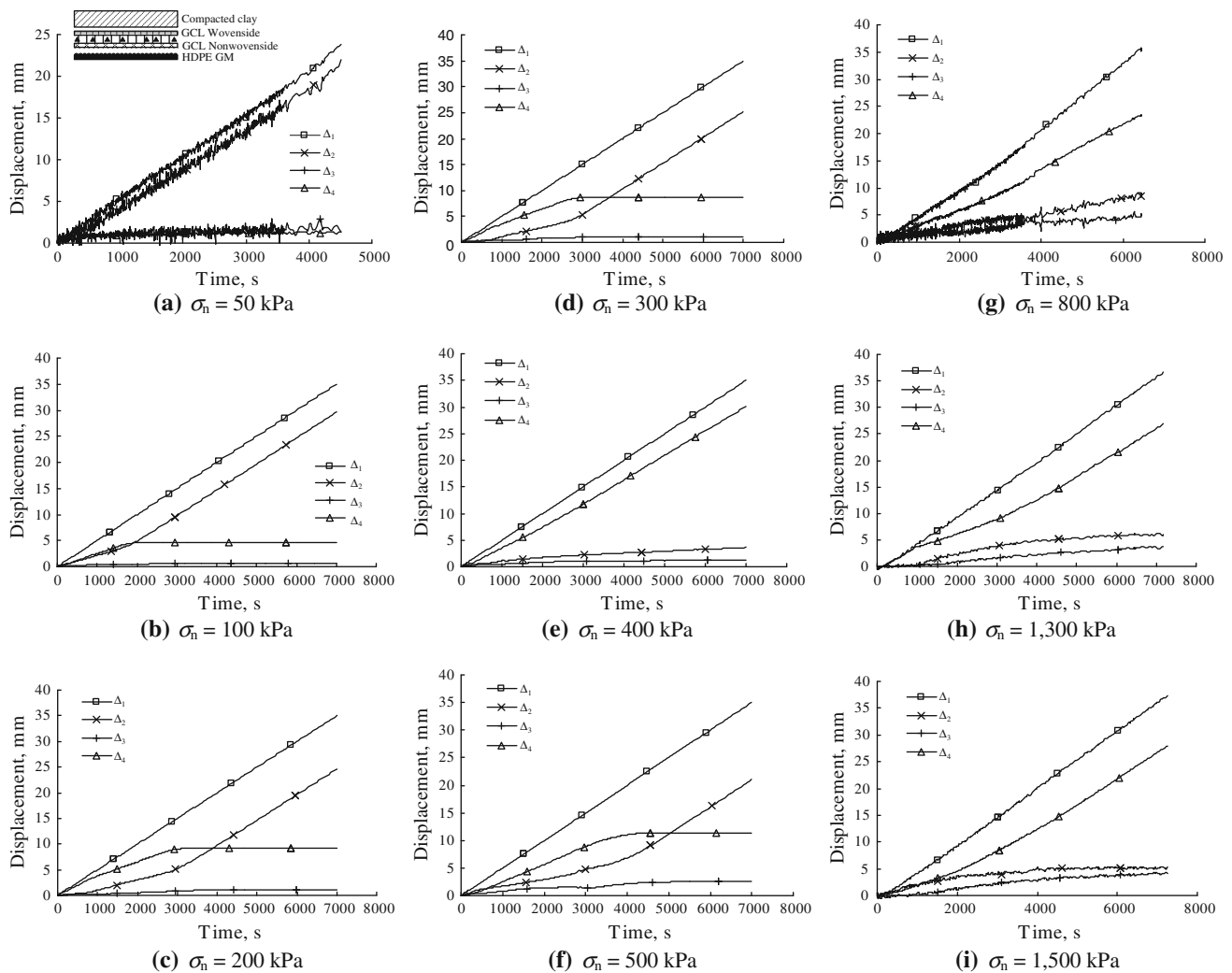


**Fig. 3** Displacement-time relationships for simple shear tests (Test Group A)

Figure 4 shows that the transition of the failure interface does not occur for Test Group B. The critical failure face is always located at the interface of WGT/GMX for all of the applied normal stresses used in the tests. No internal failure in the GCL was observed for either of the test groups in this research. This observation indicates that the internal failure will not occur when the geotextile-encased, needle-punched GCL used in the composite liner system is in dry condition.

For a composite liner system that contains two or more potential failure faces, the interface or internal displacement in the liner system occurs not only at the critical failure interface (Figs. 3 and 4). The displacement mobilized at each internal and interface in the liner system mainly depends on the shear stress-displacement relationship of each interface. It can be seen from both Figs. 3 and 4 that the displacements can be mobilized at each interface of GCL/GM and GCL/CCL and the internal face of the GCL at the beginning of shearing. The value of the

displacement at the non-critical failure face will maintain constancy after it increases to a certain “stable” value. However, the value of the displacement at the critical failure face will continuously increase with time. The “stable” value of the internal displacement in the GCL for both Test Groups A and B demonstrates approximate hyperbolic growth with increase of the normal stress (Fig. 5). Similarly, the “stable” values of the displacements at the interface of WGT/CCL for Test Group A (Fig. 3) and at the interface of NWGT/CCL for Test Group B (Fig. 4) also increase with increase of the normal stress. They are approximately equal to 11.4 mm at  $\sigma_n = 500$  kPa for Test Group A and 7.2 mm at  $\sigma_n = 1,300$  kPa for Test Group B.

#### Stress-displacement behavior

The relationships between the shear stress and the total displacement for the tested composite liners are shown in

**Fig. 4** Displacement-time relationships for simple shear tests (Test Group B)

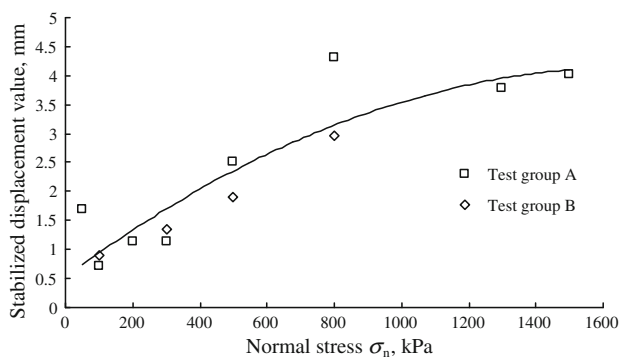
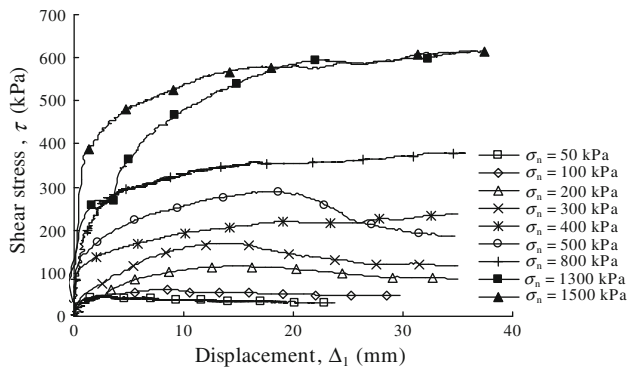


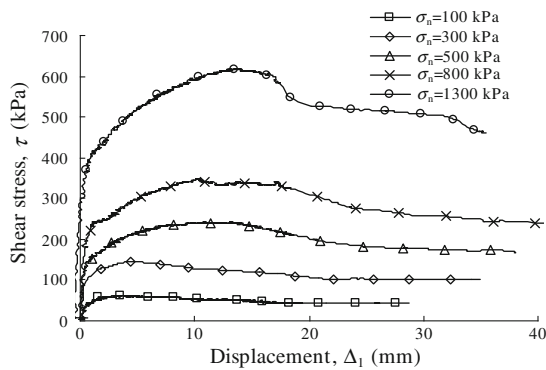
**Fig. 5** Stabilized internal displacement of GCLs

**Fig. 6.** For Test Group A, the shapes of the shear stress-total displacement curves are similar to the stress-displacement curves of the interface of NWGT/GMX for  $\sigma_n = 50, 100, 200, 300,$  and  $500$  kPa, (see Fig. 7a for  $\sigma_n = 200$  kPa). These curves have peak strength ( $\tau_p$ ) and

display a strain-softening (i.e., post-peak strength loss) behavior. The displacement corresponding to the peak strength ( $\delta_p$ ) increases with increase of the normal stress. Because of the limitation of the shearing displacement for the apparatus, the residual shear strength cannot be obtained in this study. Thus, the investigation regarding the post-peak strength behavior is not included in this study. The shear stress-total displacement curves do not display the strain-softening behavior for  $\sigma_n = 400, 800, 1,300$  and  $1,500$  kPa. The critical failure interface has changed from the interface of NWGT/GMX to the interface of WGT/CCL under these normal stresses. The shear stress-total displacement curves under these normal stresses are similar to the results of the interface of WGT/CCL from the direct shear tests conducted by Lee and Manjunath (2000). It can be seen in Fig. 6a that an extra small peak strength appears at the displacement of 3 mm for the curve of  $\sigma_n = 1,300$  kPa. It may be caused by some movement of



(a) Test Group A



(b) Test Group B

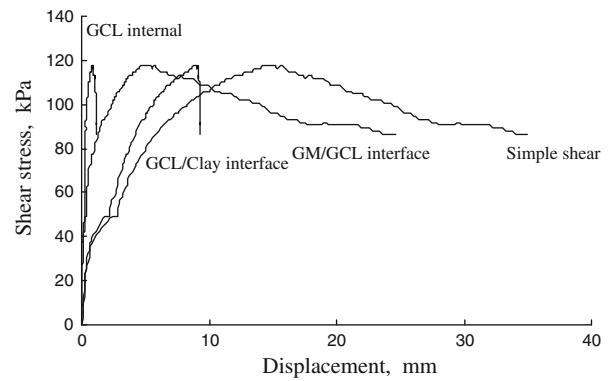
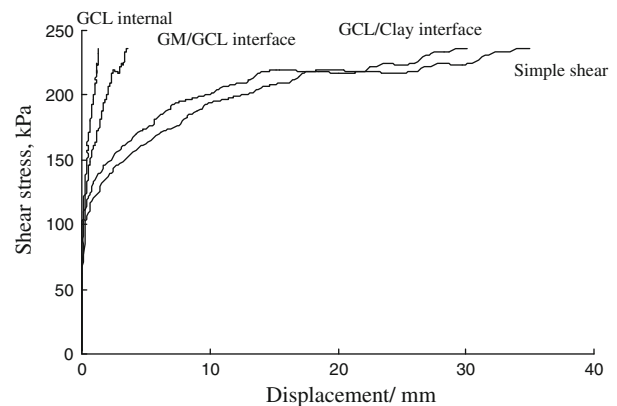
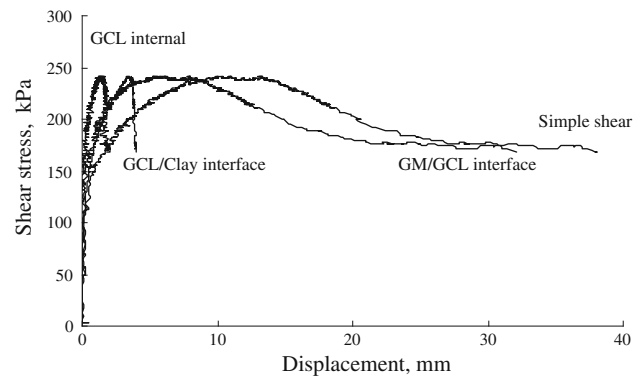
**Fig. 6** Relationship between shear stress and total displacement

the steel block in the lower shear box at the beginning of the test due to the set-up problem of the device (Fox and Kim 2008). The shear stress-total displacement curves are also similar to the stress-displacement curves of the interface of WGT/CCL for  $\sigma_n = 400, 800, 1,300,$  and  $1,500$  kPa (see Fig. 7b for  $\sigma_n = 400$  kPa).

For Test Group B, the shapes of all of the shear stress-total displacement curves are similar to the stress-displacement curves of the interface of WGT/GMX for all normal stresses (see Fig. 7c for  $\sigma_n = 500$  kPa). All of these curves have peak strength ( $\tau_p$ ) and demonstrate strain-softening behavior. The displacement corresponding to the peak strength ( $\delta_p$ ) increases with increase of the normal stress. Failure always occurs at the interface of WGT/GMX for  $\sigma_n = 100, 300, 500, 800$  and  $1,300$  kPa.

#### Peak strength and failure mode

The peak shear strengths at the critical failure interface under various normal stresses for both Test Groups A and B are plotted in Fig. 8. The test results adopted from Chiu and Fox (2004) and Triplett and Fox (2001) are also plotted in Fig. 8 to make comparisons. Figure 8 shows that the peak failure envelope for Test Group A is linear when the critical failure interface is located at the interface of

(a) Test series (A) at  $\sigma_n = 200$  kPa(b) Test series (A) at  $\sigma_n = 400$  kPa(c) Test series (B) at  $\sigma_n = 500$  kPa**Fig. 7** Shear stress-displacement relationships for each interface during shearing

NWGT/GMX for  $\sigma_n = 50, 100, 200,$  and  $300$  kPa. The peak failure envelope for Test Group A becomes non-linear when the critical failure interface is located at the interface of WGT/CCL for  $\sigma_n = 800, 1,300,$  and  $1,500$  kPa. It indicates that the friction angle at the failure interface decreases with increase of the normal stress. For Test Group B, the critical failure interface is always located at the interface of WGT/CCL for all normal stresses. The peak failure envelope for Test Group B is lower than that for Test Group A when  $\sigma_n \leq 500$  kPa (Fig. 8). The peak



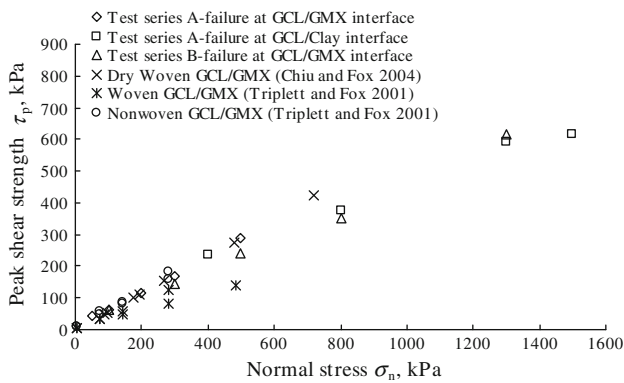


**Fig. 8** Peak strength envelopes for GCL interfaces

failure envelope for Test Group B can be well simulated by a linear regression equation as follows:

$$\tau_p = 7.4 \text{ kPa} + \sigma_n \tan 24.6^\circ \tag{1}$$

It can be seen in Fig. 8 that the peak strength envelope for Test Group B is slightly lower than the peak strengths at the dry interface of WGT/GMX from the direct shear tests conducted by Chiu and Fox (2004). The difference in the results may be due to the testing materials (such as GCL and GM) made by different manufacturers and the usage of different testing devices (i.e., simple and direct shear apparatuses). When the normal stress is low ( $\sigma_n = 100 \sim 300$  kPa), the peak strengths of the NWGT/GMX interface from Test Groups A and the WGT/GMX interface from Test Group B are close to that of the GCL NWGT/GMX interface and the GCL WGT/GMX interface tested by Triplet and Fox (2001), respectively. However, the peak strength envelope of the WGT/GMX interface from Test Group B is much higher than that of the WGT/GMX interface as per Triplet and Fox (2001) when  $\sigma_n > 300$  kPa. The GCL tested by Triplet and Fox (2001) was fully hydrated by water. The mechanisms of the shear strength of the GCL WGT/GM interface are complex combinations of friction, hook and loop, and lubrication of hydrated bentonite (Hebeler et al. 2005; Vukelić et al. 2008; Chen et al. 2010). Hydration may have little effect on the peak strength of the GCL WGT/GM interface under low normal stress. However, for a hydrated GCL, bentonite extrusion will increase with the increases of the normal stress, and the lubrication effect of bentonite at the GCL interface may cause reduction of the interface strength. Vukelić et al. (2008) reported that the bentonite extrusion did not affect the peak strength of the GCL/GM interface in dry condition. Vukelić et al. (2008) also found that the bentonite extrusion was approximately zero when  $\sigma_n < 100$  kPa and GCL hydration does not affect the peak interface strength under low normal stress. This is similar to the results presented above.

Eid (2011) used a torsional ring shear apparatus to provide simultaneous shearing tests for a GCL composite liner. The test results revealed that the critical failure interfaces of a composite can change with the normal stress. The test results also revealed three critical failure interfaces for a composite liner consisting of textured geomembrane, hydrated GCL, and compacted clay. In this tested composite liner system, the location of the shear failure surface depends on the magnitude of the applied normal stress. There are three failure modes for this composite liner system. The composite specimen fails along the interface of NWGT/CCL when  $\sigma_n \leq 75$  kPa, and along the interface of WGT/GMX when  $\sigma_n = 100\text{--}250$  kPa, and through shearing of the GCL internally when  $\sigma_n \geq 300$  kPa. Fox and Ross (2011) also found that the failure mode for the tested specimens consisting of the textured geomembrane and hydrated needle-punched GCL can change interface shear between NWGT side of the GCL and Textured GM (i.e., NWGT/GMX) to internal shear of the GCL as normal stress increases. Failure mode transition occurred around the normal stress of 1,382 kPa. Both the test results from Eid (2011) and Fox and Ross (2011) show that a GCL composite specimen can fail through shearing of the GCL internally as normal stress increases. However, internal shear failure of the GCL was not observed even when the normal stresses were increased to 1,500 kPa for Test Group A and 1,300 kPa for Test Group B in this study. That may be due to the difference in GCLs used in each study. Hydrated GCLs were used by Eid (2002) and Fox and Ross (2011) and dry GCL was used in this study. Given that the hydrated bentonite has a very low internal friction angle (e.g.,  $7^\circ \sim 9^\circ$ ; Daniel et al. 1993), the internal shear strength for a hydrated needle-punched reinforced GCL is mainly contributed by the needle-punched fibers in the GCL. However, the internal friction angle for dry bentonite can be up to  $27^\circ\text{--}36^\circ$  (Daniel et al. 1993). The internal shear strength for a dry needle-punched reinforced GCL should be the combination of the shear strengths of both dry bentonite and needle-punched fibers in the GCL. It is much greater than the internal strength of hydrated GCL and the interface strength between the GCL and textured geomembrane or compacted clay. This may be the reason why internal failure did not occur for a dry GCL composite specimen at a high normal stress.

**Conclusions**

With respect to the issue of investigation of shearing behavior of GCL composite liner systems by using a large improved simple shear apparatus, the following conclusions are offered:

1. The large improved simple shear apparatus used in this study does not force the shear failure to occur along a pre-determined plane. The composite specimens can fail along the GM/GCL interface, GCL/CCL interface, or through shearing of the GCL internally. Simultaneous shearing of a composite liner specimen that contains several components affected by the same testing conditions helps in simulating the field condition more than testing the shear strength of each interface individually. Another advantage of this apparatus is that the displacement of each component of a composite liner specimen can be measured during the tests.
2. When the non-woven geotextile side of the GCL comes in contact with the textured geomembrane (NWGT/GMX) and the woven geotextile side of the GCL comes in contact with the compacted clay layer (WGT/CCL) (i.e., Test Group A), failure occurs at the interface of NWGT/GMX when the normal stress is <400 kPa. The critical failure face shifts to the interface of WGT/CCL interface when the normal stress is greater than 500 kPa. When the normal stress changes between 400 and 500 kPa, failure may occur at the interface of either NWGT/GMX or WGT/CCL. Conversely, when the woven geotextile side of GCL comes in contact with textured GM (WGT/GMX) and the non-woven geotextile side of GCL comes in contact with the compacted clay layer (NWGT/CCL) (i.e., Test Group B), failure always occurs at the interface of WGT/GMX even when the normal stress is up to 1,300 kPa.
3. Internal shear failure of the GCL for a dry GCL composite specimen did not occur even when the normal stresses were increased up to 1,500 kPa for Test Group A and 1,300 kPa for Test Group B in this study. It indicates that the internal shear strength for a dry needle-punched reinforced GCL is much greater than the interface strength between the GCL and textured geomembrane or compacted clay.
4. For a composite liner system that may contain two or more potential failure faces, the displacement in the liner system does not occur only at the failure face. The simple test results showed that displacement can be mobilized at each interface and internal face of the GCL. The mobilized displacement mainly depends on the shear stress-displacement relationship of each face in the liner. The values of the normal stress corresponding to the transition of the failure face can be determined from the displacement behavior for each interface in the liner system. The internal displacement of the GCL increases non-linearly as the normal stress increases. The internal displacement of the GCL maintains a small value (<10 mm) under the entire normal stresses used in this research.
5. The peak failure envelope for Test Group B is linear for the entire stress range and the tangential friction angle is 24.6°. The peak failure envelope for Test Group A is non-linear and indicates that the friction angle decreases with the increase of the normal stress. When the normal stress is less than 500 kPa, the peak strength obtained from Test Group A is greater than that obtained from Test Group B.

A hydrated GCL will be used in future research. In addition, a composite specimen such as the portion of a double composite liner system, which consists of textured geomembrane (i.e., primary geomembrane), reinforced GCL (i.e., primary clay liner), and geocomposite drainage layer (i.e., leak detection layer), will also be selected in future research.

**Acknowledgments** The authors appreciate the financial support provided by National Natural Science Foundation of China (No. 41172234).

**Open Access** This article is distributed under the terms of the Creative Commons Attribution License which permits any use, distribution, and reproduction in any medium, provided the original author(s) and the source are credited.

## References

- Anderson R, Rayhani MT, Rowe RK (2012) Laboratory investigation of GCL hydration from clayey sand subsoil. *Geotext Geomembr* 31(1):31–38
- ASTM D 6243-09 (2009) Standard Test Method for Determining the Internal and Interface shear resistance of Geosynthetic Clay Liner by the Direct Shear Method, American Society for Testing and Materials, West Conshohocken, Pennsylvania, USA
- Bouazza A (2002) Geosynthetic clay liners. *Geotext Geomembr* 20(1):3–17
- Chen YM, Lin WA, Zhan LT (2010) Investigation of mechanisms of bentonite extrusion from GCL and related effects on the shear strength of GM/GCL interfaces. *Geotext Geomembr* 28(1): 63–71
- Chiu P, Fox PJ (2004) Internal and interface shear strengths of unreinforced and needle-punched geosynthetic clay liners. *Geosynth Int* 11(3):176–179
- CJJ 113-2007 (2007) Technical code for liner system of municipal solid waste landfill, Ministry of Construction of the People's Republic of China, China Building Industry Press, Beijing, China
- Daniel DE, Shan HY, Anderson JD (1993) Effects of partial wetting on the performance of the Bentonite component of a Geosynthetic clay liner. In: Proceedings of geosynthetics '93, vol. 3, Vancouver, March 1993, Industrial Fabrics Association International, St. Paul, MN, pp 1483–1496
- Dixon N, Jones DRV, Fowmws GJ (2006) Interface shear strength variability and its use in reliability-based landfill stability analysis. *Geosynth Int* 13(1):1–14
- Eid HT (2011) Shear strength of geosynthetic composite systems for design of landfill liner and cover slopes. *Geotext Geomembr* 29(3):335–344
- Eid HT, Stark TD (1997) Shear behavior of an unreinforced geosynthetic clay liner. *Geosynth Int* 4(6):645–659

- Eid HT, Stark TD (1999) Effect of shear displacement rate on internal shear strength of a reinforced geosynthetic clay liner. *Geosynth Int* 6(3):219–239
- Fox PJ, Kim RH (2008) Effect of progressive failure on measured shear strength of geomembrane/GCL interface. *J Geotech Geoenvironmental Eng* 134(4):459–469
- Fox PJ, Ross JD (2011) Relationship between NP GCL internal and HDPE GMX/NP GCL interface shear strengths. *J Geotech Geoenvironmental Eng* 137(8):743–753
- Fox PJ, Stark TD (2004) State-of-the-art report: GCL shear strength and its measurement. *Geosynth Int* 11(3):141–175
- Fox PJ, Rowland MG, Scheithe JR (1998) Internal shear strength of three geosynthetic clay liners. *J Geotech Geoenvironmental Eng* 124(10):933–944
- Gilbert RB, Fernandez F, Horsfield DW (1996) Shear strength of reinforced geosynthetic clay liner. *J Geotech Geoenvironmental Eng* 122(4):259–265
- Hebeler GL, Frost JD, Myers AT (2005) Quantifying hook and loop interaction in textured geomembrane-geotextile systems. *Geotext Geomembr* 23(1):77–105
- ISO/TS 17892-10-2004 (2004) Geotechnical investigation and testing-Laboratory testing of soil-Part 10: Direct shear tests
- Koerner RM, Soong TY (2000) Stability Assessment of Ten Large Landfill Failures. *Advances in Transportation and Geoenvironmental Systems Using Geosynthetics, Proceedings of Sessions of GeoDenver 2000, ASCE Geotechnical Special Publication (GSP) No. 103*, 1–38
- Lee KM, Manjunath VR (2000) Soil-geotextile interface friction by direct shear tests. *Can Geotech J* 37(1):238–252
- McCartney JS, Zornberg JG, Swan JRH (2009) Analysis of a large database of GCL-geomembrane interface shear strength results. *J Geotech Geoenvironmental Eng* 135(2):209–223
- Qian X, Koerner RM, Gray DH (2002) Geotechnical aspects of landfill design and construction, chap 18, Prentice Hall Inc., Upper Saddle River
- Ross JD, Fox PJ, Olsta JT (2011) Dynamic shear response of a geomembrane/geosynthetic clay liner interface. *Geo-Frontiers: 2010–2020*
- Triplett EJ, Fox PJ (2001) Shear strength of HDPE geomembrane/geosynthetic clay liner interfaces. *J Geotech Geoenvironmental Eng* 127(6):543–552
- Vukelić A, Szavits-Nossan A, Kvasnička P (2008) The influence of bentonite extrusion on shear strength of GCL/geomembrane interface. *Geotext Geomembr* 26(1):82–90
- Zornberg JG, McCartney JS, Swan JRH (2005) Analysis of a large database of GCL internal shear strength results. *J Geotech Geoenvironmental Eng* 131(3):367–380